Absorption signatures of the heliosphere

Brian E. Wood*, Vladislav V. Izmodenov† and Nikolai V. Pogorelov**

*JILA, University of Colorado, Boulder, CO 80309-0440, USA
†Lomonosov Moscow State University, Dept. of Aeromechanics and Gas Dynamics, Moscow 119899, Russia
**Institute of Geophysics and Planetary Physics, University of California at Riverside, 900 University Avenue, Riverside, CA 92521, USA

Abstract. Observations of stellar H I Lyman-α lines from the Hubble Space Telescope have provided many absorption detections of neutral H in the outer heliosphere. There have recently been new detections of heliospheric absorption, and we have begun to use this additional data in combination with older detections to provide more thorough tests of heliospheric models, including new 3D models that include the effects of the interstellar magnetic field. We find that the heliospheric Lyman-α absorption predicted by the models is modestly affected by both the magnitude and orientation of the assumed ISM magnetic field, so there is potential for the absorption to provide constraints on the nature of the interstellar field in the solar neighborhood.

Keywords: HST, Lyman-α absorption, heliosphere, ISM
PACS: 95.55.Fw, 96.50.Ek, 96.50.Xy, 98.38.-j

INTRODUCTION

Voyager 1's crossing of the termination shock has opened up a whole new region of the heliosphere for exploration, namely the heliosheath between the termination shock and heliopause. However, the outermost areas of the solar wind/ISM interaction region beyond the heliopause still remain mostly inaccessible. The only direct observational diagnostics of material in these remote regions are absorption features in high resolution spectra of stellar Lyman-α lines, which are observed by the Hubble Space Telescope (HST). The hot hydrogen that permeates the heliosphere thanks to charge exchange interactions is capable of producing detectable Lyman-α absorption for observed lines of sight through the heliosphere to nearby stars, at least in cases where the ISM absorption is not too strong to obscure the heliospheric signal. For all but the most downwind directions the heliospheric absorption will be dominated by the so-called "hydrogen wall" region between the heliopause and bow shock, where interstellar hydrogen has been heated, compressed, and decelerated.

From the first detection of heliospheric Lyman-α absorption towards α Cen [1], the absorption diagnostic has proved useful for testing hydrodynamic models of the global heliosphere. The detected absorption represents a confirmation of the existence of the hydrogen wall, which was predicted by the first models to treat the ISM neutrals and the ambient plasma in a self-consistent manner [2, 3, 4]. Various analyses have demonstrated that such models are generally successful in reproducing the observed absorption [5, 6, 7].

However, the exact amount of absorption predicted by the models is dependent on the

CP 858, *Physics of the Inner Heliosheath,*
edited by J. Heerikhuisen, V. Florinski, G. P. Zank, and N. V. Pogorelov

precise parameters that are assumed for the undisturbed ISM surrounding the Sun. Some of these properties are known very well, such as the ISM flow velocity and direction; but others, such as the proton and neutral H number densities, are not known as precisely. Thus, there has been hope that the Lyman-α absorption can provide constraints on these values. Hampering these assessments are problems with model dependence and only a modest sensitivity of the absorption to many input parameters of interest [7].

NEW HELIOSPHERIC ABSORPTION DETECTIONS

The first data/model comparison involving the Lyman-α absorption considered only the α Cen line of sight [5]. Subsequent Lyman-α analyses yielded new heliospheric absorption detections for the lines of sight to Sirius [8] and 36 Oph [9]. Thus, more recent comparisons of observed Lyman-α absorption with model predictions have considered all three detections in order to constrain the models in different directions [6, 7]. In order to more fully sample the range of angles from upwind to downwind, these analyses also considered three additional lines of sight without heliospheric detections, which provide upper limits for the absorption in those directions.

However, this sample is still rather small to constrain even the axisymmetric models that have been used in the past. The situation is even worse for the real heliosphere, where magnetic field effects and a latitude-dependent solar wind will drive the heliosphere away from a purely axisymmetric structure. Greater computing power and model sophistication has allowed theorists to start constructing true 3D models of the heliosphere that include the effects of magnetic fields [10, 11, 12]. For the Lyman-α absorption to properly constrain models of the real three-dimensional heliosphere requires a larger number of observed lines of sight distributed over all sky directions.

Fortunately, the number of absorption detections has by now increased from three to eight, mostly due to a systematic search through the HST archives for Lyman-α spectra of nearby stars [13]. Figure 1 shows a sky map of HST-observed lines of sight in ecliptic coordinates. The figure shows that the eight lines of sight with detected heliospheric absorption are mostly near the upwind direction of the ISM flow vector. Detections are simply easier in upwind directions since that is where the deceleration of the ISM flow is strongest, which shifts the heliospheric absorption away from the ISM absorption, making it easier to detect.

Our goal is to select from the observed lines of sight in Figure 1 a sample of Lyman-α spectra to compare with model predictions. Obviously, we choose the 8 lines of sight with actual heliospheric detections, and we supplement these data with 10 lines of sight with nondetections, which can at least provide upper limits for heliospheric absorption. The nondetections are chosen to cover the sky as much as possible (see Fig. 1). We also preferentially select spectra with high data quality and lines of sight with low ISM column densities, since a low ISM column means less ISM absorption and lower upper limits for the amount of heliospheric absorption that can be present.

The final sample of 18 lines of sight are indicated in Figure 1 as numbered symbols. Figure 2 identifies these stars and shows the red side of the Lyman-α absorption profile where the heliospheric absorption is detected, when present. (See [13] and references therein for the full spectra.) The spectra are presented in order of increasing distance

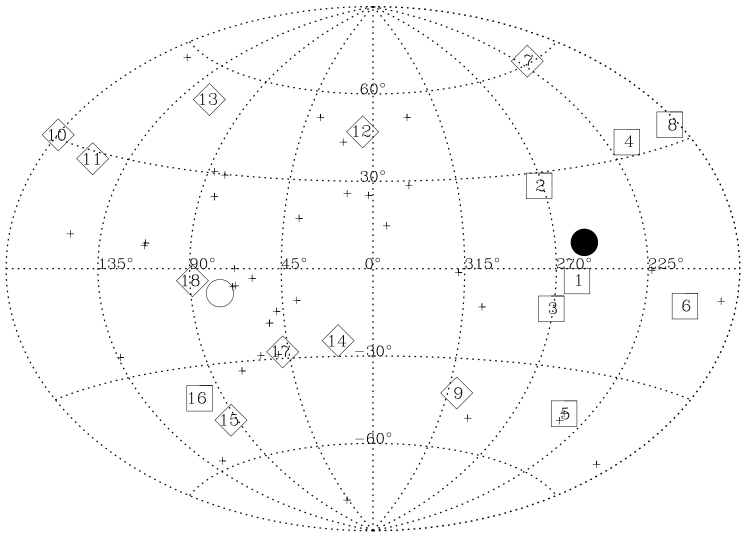

FIGURE 1. Sky map in ecliptic coordinates of all HST-observed lines of sight with useful Lyman-α spectra. The numbered symbols indicate spectra that we will compare with model predictions (see Fig. 2). Boxes indicate lines of sight with detected heliospheric absorption, while diamonds are other selected lines of sight that are nondetections but will still provide upper limits for absorption in those directions. The filled and open circles indicate the upwind and downwind direction of the ISM flow vector, respectively.

from the upwind direction. Dotted lines show the ISM absorption alone for these lines of sight. For the 8 lines of sight with detections of heliospheric absorption, there is excess absorption observed beyond that from the ISM that models can attempt to reproduce. For the 10 nondetections, the ISM absorption fits the data reasonably well by itself and successful heliospheric models should ideally predict no additional absorption beyond that from the ISM.

CONSTRAINING THE INTERSTELLAR MAGNETIC FIELD

The nature of the interstellar magnetic field surrounding the Sun is poorly known. The global Galactic field has a magnitude of 1.6 ± 0.2 μG and is directed towards a Galactic longitude of $l = 96 \pm 4°$, but there is substantial local variability [14], meaning that the actual local field could be significantly higher or lower and could be in a completely different direction. Lallement et al. [15] reported a discrepancy between the flow vectors of interstellar He and H within the solar system, and proposed that this is due to an ISM magnetic field that is skewed with respect to the ISM flow direction, which can deflect the flow of interstellar hydrogen atoms in the heliosphere. Helium atoms are not affected in this manner, since their charge exchange cross sections are much lower than hydrogen and they are therefore effectively blind to the presence of the heliosphere. If correct, this interpretation identifies a plane in which the ISM field can lie.

Properly considering the effects of the ISM field on the heliosphere requires a fully

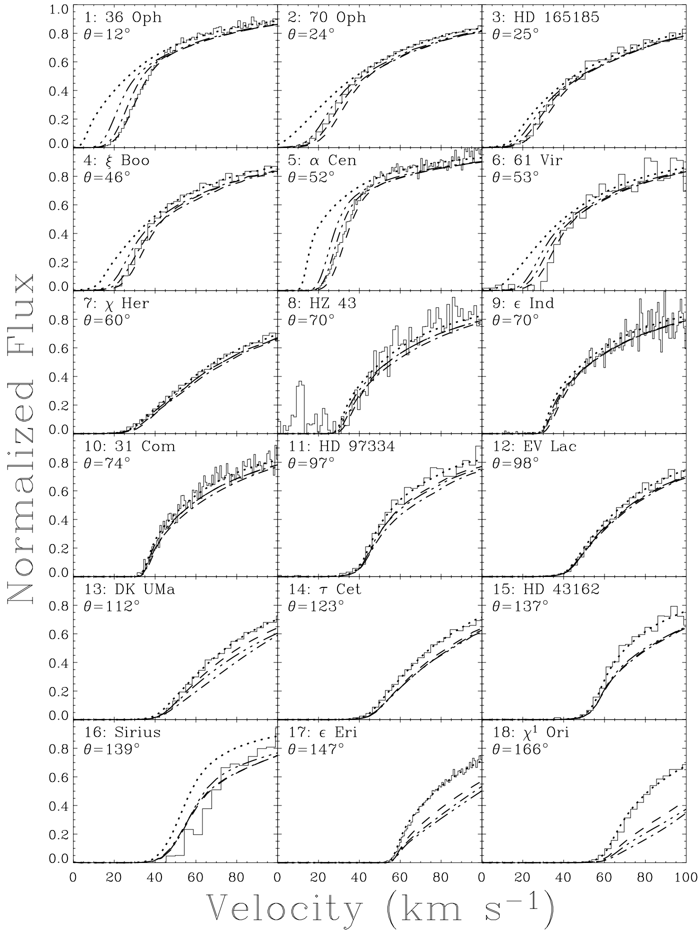

FIGURE 2. The red side of the Lyman-α absorption line for the selected stars from Fig. 1, where the stars are placed in order of increasing angle from the upwind direction of the ISM flow (θ). In each panel, the dotted line is the ISM absorption alone. Absorption predictions are shown for heliospheric models computed assuming ISM field orientations of $\alpha = 0°$ (dashed line), $\alpha = 45°$ (dot-dashed line), and $\alpha = 90°$ (3-dot-dashed line).

3D model, except for the special case of a field parallel to the ISM flow [16]. Three dimensional models that include an ISM field and also model neutral hydrogen in a self-consistent manner with the plasma have only recently become available. Thus, for the first time we can see if the Lyman-α absorption should be sensitive to the strength and orientation of the ISM magnetic field.

Izmodenov et al. [11] have expanded the Baranov & Malama [3] heliospheric modeling code, which uses a full kinetic treatment of neutral hydrogen in the heliosphere, into a fully 3D code that includes the ISM magnetic field. A set of models has been computed assuming an ISM field strength of $B = 2.5\ \mu$G. The orientation of the field, defined by the angle (α) between the field direction and the ISM flow vector, is varied within the plane defined by Lallement et al. [15]. The ISM hydrogen and proton densities assumed in these models are $n_H = 0.18$ cm^{-3} and $n_p = 0.06$ cm^{-3}, and the temperature is assumed to be $T = 6400$ K.

Figure 2 shows the Lyman-α absorption predicted by models with α=0°, 45°, and 90°. In upwind directions, where most of the heliospheric detections are, the absorption decreases with increasing α. The $\alpha = 90°$ model underestimates the absorption in all cases, so perhaps this model should be ruled out. It is not entirely clear whether the $\alpha = 0°$ or $\alpha = 45°$ model is better, since $\alpha = 0°$ seems to work best for some lines of sight (36 Oph, 61 Vir) and $\alpha = 45°$ works best for others (70 Oph, ξ Boo, α Cen). The observed H flow deflection [15] would argue against $\alpha = 0°$ and for $\alpha = 45°$, which is in fact a model that reproduces the observed deflection [11]. It should be stated that definitive conclusions are difficult to make at this point since the Lyman-α absorption is at least somewhat sensitive to other input parameters, such as the assumed ISM densities and temperature. A time-consuming thorough exploration of parameter space would be necessary to fully characterize the constraints provided by Lyman-α absorption.

We also note the apparent overprediction of absorption in downwind directions (see Figure 2). This has been observed for other models with a fully kinetic treatment of the neutrals [6, 7]. This downwind absorption is not from the hydrogen wall, but from the heliosheath. Unlike the comparatively sharp and saturated hydrogen wall absorption seen in upwind directions, the heliosheath absorption predicted by the models is very broad and unsaturated. It is difficult to observationally rule out the existence of such absorption, because one can in principle alter the assumed stellar Lyman-α emission profile to allow it to exist [6, 7]. Thus, it is not clear at this point whether the apparent downwind discrepancies with the data, particularly for ε Eri and χ^1 Ori, are large enough to imply a fundamental problem with these models. We hope to address these downwind issues in detail in a future paper.

Pogorelov et al. [12] have also developed a code for computing 3D MHD models of the heliosphere. This code uses a less sophisticated 2-fluid treatment for the neutral H velocity distributions, but it includes the effects of the interplanetary magnetic field on heliospheric structure as well as the ISM field. Like the models used in Figure 2, models computed using this code also indicate that Lyman-α absorption decreases with increasing α.

Figure 3 shows the absorption predictions of two of these 2-fluid models assuming different ISM field strengths of $B = 1.5\ \mu$G and $B = 4.0\ \mu$G. The field orientations of these models are also slightly different, with the low field model having $\alpha = 0°$ and the high field model assuming $\alpha = 15°$. We only show the predicted absorption for four of the upwind lines of sight with detected heliospheric absorption. Figure 3 suggests that increasing the ISM field strength significantly decreases the amount of absorption, though part of the decrease could be from the increase in α. Both of these particular models actually underpredict the amount of observed absorption, perhaps because these particular models assume rather low values for the ISM density and temperature ($n_H = 0.1$ cm^{-3}, $n_p = 0.07$ cm^{-3}, $T = 5680$ K). Regardless, these results suggest that the Lyman-α absorption will be sensitive to ISM field strength as well as orientation. A more extensive parameter survey is necessary to quantify these effects.

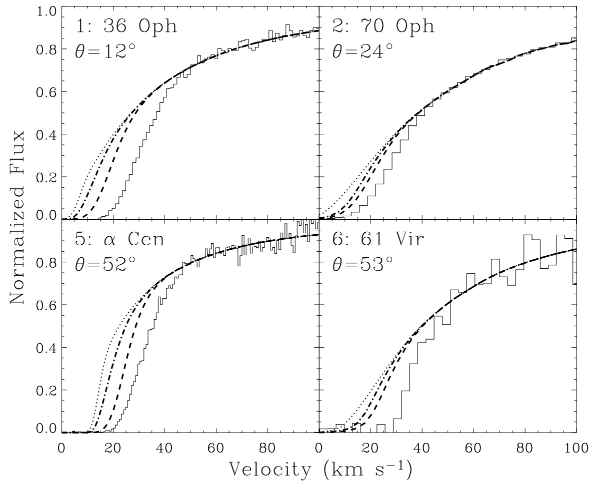

FIGURE 3. The red side of the Lyman-α absorption line for four of the stars from Fig. 1, where the stars are in order of increasing angle from the upwind direction of the ISM flow (θ). In each panel, the dotted line is the ISM absorption alone. Absorption predictions are shown for heliospheric models computed assuming an ISM field strength of $B = 1.5\ \mu$G (dashed line) and $B = 4.0\ \mu$G (dot-dashed line).

ACKNOWLEDGMENTS

Support for this work was provided by NASA through grant NNG05GD69G to the University of Colorado.

REFERENCES

1. J. L. Linsky, and B. E. Wood, *Astrophys. J.* **463**, 254–270 (1996).
2. V. B. Baranov, M. G. Lebedev, and Y. G. Malama, *Astrophys. J.* **375**, 347–351 (1991).
3. V. B. Baranov, and Y. G. Malama, *J. Geophys. Res.* **100**, 14,755–14,762 (1995).
4. G. P. Zank, H. L. Pauls, L. L. Williams, and D. T. Hall, *J. Geophys. Res.* **101**, 21,639–21,656 (1996).
5. K. G. Gayley, G. P. Zank, H. L. Pauls, P. C. Frisch, and D. E. Welty, *Astrophys. J.* **487**, 259–270 (1997).
6. B. E. Wood, H. -R. Müller, and G. P. Zank, *Astrophys. J.* **542**, 493–503 (2000).
7. V. V. Izmodenov, B. E. Wood, and R. Lallement, *J. Geophys. Res.* **107**, 1308–1322 (2002).
8. V. V. Izmodenov, R. Lallement, and Y. G. Malama, *Astron. Astrophys.* **342**, L13–L16 (1999).
9. B. E. Wood, J. L. Linsky, and G. P. Zank, *Astrophys. J.* **537**, 304–311 (2000).
10. M. Opher, P. C. Liewer, T. I. Gombosi, W. Manchester, D. L. DeZeeuw, I. Sokolov, and G. Toth, *Astrophys. J.* **591**, L61–L65 (2003).
11. V. Izmodenov, D. Alexashov, and A. Myasnikov, *Astron. Astrophys.* **437**, L35–L38 (2005).
12. N. V. Pogorelov, and G. P. Zank, *Astrophys. J.* **636**, L161–L164 (2006).
13. B. E. Wood, S. Redfield, J. L. Linsky, H. -R. Müller, and G. P. Zank, *Astrophys. J. Suppl.* **159**, 118–140 (2005).
14. R. J. Rand, and S. R. Kulkarni, *Astrophys. J.* **343**, 760–772 (1989).
15. R. Lallement, E. Quémerais, J. L. Bertaux, S. Ferron, D. Koutroumpa, and R. Pellinen, *Science* **307**, 1447–1449 (2005).
16. V. Florinski, N. V. Pogorelov, G. P. Zank, B. E. Wood, and D. P. Cox, *Astrophys. J.* **604**, 700–706 (2004).